

ANISOTROPIC OPTICAL REFLECTANCE OF $\text{Hg}_{2.86}\text{AsF}_6$

ANISOTROPIC OPTICAL REFLECTANCE

OF $\text{Hg}_{2.86}\text{AsF}_6$

By

ERWIN BATALLA, B.Sc.

A Thesis

Submitted to the School of Graduate Studies

in Partial Fulfilment of the Requirements

for the Degree

Master of Science

McMaster University

September 1976

MASTER OF SCIENCE (1976)
(Physics)

McMASTER UNIVERSITY
Hamilton, Ontario

TITLE: Anisotropic Optical Reflectance of $\text{Hg}_{2.86}\text{AsF}_6$

AUTHOR: Erwin Batalla, B.Sc. (Montreal University)

SUPERVISOR: Dr. W. R. Datars

NUMBER OF PAGES: vi, 31

SCOPE AND CONTENTS:

Optical reflectance of the quasi two dimensional compound $\text{Hg}_{2.86}\text{AsF}_6$ has been investigated in the optical range, 0.5 to 4 eV. The spectra clearly show a plasma edge at 3 eV. They are fitted to a Drude model and two Lorentz oscillators. From the plasma frequency and the model parameters values for the dc conductivity and the effective mass and an estimate of the crystal anisotropy have been obtained. The results compare well with earlier electrical measurements on this compound.

ACKNOWLEDGEMENTS

I should like to thank my supervisor, Dr. W. R. Datars, for his advice and assistance during the course of the work and in the writing of this thesis. Many others have aided me in this work. I acknowledge the cooperation of Dr. Gillespie and the help of Dr. B. D. Cutforth and Duane Chartier who produced and mounted the crystals. I am very grateful to Dr. E. S. Kotales for setting up the apparatus. I also thank Dr. Z. Altounian for his considerable help in the writing of this thesis. I thank Dr. Timusk for the use of his spectrometer. I also acknowledge the help of all the other members of Dr. Datars' group. Finally, I should like to thank K. Overholt for her swift and accurate typing of this thesis.

This research was supported through grants from the National Research Council of Canada.

TABLE OF CONTENTS

| CHAPTER | | PAGE |
|---------|------------------------------|------|
| I | INTRODUCTION | 1 |
| II | STRUCTURE OF THE COMPOUND | 3 |
| III | THEORY OF OPTICAL REFLECTION | 6 |
| IV | EXPERIMENTAL METHOD | 14 |
| | A. Sample Preparation | 14 |
| | B. Apparatus | 14 |
| V | RESULTS | 20 |
| | A. Experimental Results | 20 |
| | B. Analysis | 23 |
| VI | DISCUSSION | 27 |
| VII | CONCLUSION | 30 |
| | BIBLIOGRAPHY | 31 |

LIST OF FIGURES

| FIGURE NO. | | PAGE |
|------------|---|------|
| 1 | Isometric view of $\text{Hg}_{2.86}\text{AsF}_6$ | 5 |
| 2 | Test tube used for sample preparation | 15 |
| 3 | Top-view of the reflectivity apparatus | 18 |
| 4 | Reflectivity as a function of time in the dry box | 21 |
| 5 | Reflectivity spectrum of the high conductivity direction | 24 |
| 6 | Reflectivity spectrum for light polarized along axis 3 | 25 |

LIST OF TABLES

| TABLE NO. | | PAGE |
|-----------|--|------|
| 1 | Crystal data for $\text{Hg}_{2.86}\text{AsF}_6$ | 4 |
| 2 | Description of ranges for the reflectivity spectrum | 17 |

CHAPTER I

INTRODUCTION

In the last few years, there has been a great deal of research on one-dimensional metallic compounds. This interest exists because it is suggested (Little, 1964) that these compounds could possess a high superconducting transition temperature and secondly, there are several phenomena that are particular to one-dimensional systems: for example, the Peierls transition and the Frölich collective mode. Therefore, there has been considerable research on such compounds as $(\text{SN})_x$, TKNQ salts and square-planar platinum complex (KCP) (Schuster, 1974).

One more system which shows one-dimensional properties (Cutforth *et al*, 1976) has been synthesized in our Chemistry department. It is a group of polycations of mercury in which there are infinite chains of this element running through a tetragonal lattice of arsenic or antimony hexafluoride octahedra (Brown *et al*, 1974). Those chains are continuous in two directions giving the compound considerable anisotropy in its properties.

The conductivity of $\text{Hg}_{2.91}\text{SbF}_6$ and $\text{Hg}_{2.86}\text{AsF}_6$ has been measured from 4 to 300 K (Cutforth *et al*, 1976). They found that the conductivity increases steadily as the temperature is reduced as is expected for a normal metal. The room-temperature conductivity for both compounds is of the order of $10^4 (\Omega \times \text{cm})^{-1}$ and the ratio of the resistivity at room-temperature to the resistivity at liquid helium temperature is about 1000

in the high conductivity direction. The anisotropy is relatively constant at a value of approximately 100.

Also, differential thermal analysis (D.T.A.) has shown that both compounds go through some kind of transition at about 235 K (van Schyndel et al., 1976). This is confirmed by an anomaly in the conductivity data.

Finally, the reflectivity of $\text{Hg}_{2.91}\text{SbF}_6$ has been studied at room-temperature (Koteles et al., 1976). A plasma edge has been found and the whole spectrum was fitted to a Drude model and two Lorentz oscillators. The parameters from the fit give a value of the conductivity slightly lower than the observed one at room-temperature and a high value for the effective mass.

In this work, the reflectivity of $\text{Hg}_{2.86}\text{AsF}_6$ is measured in the visible and the near infrared. The results of these experiments are then fitted using a classical Drude model and some Lorentz oscillators. From the parameters obtained in this way (plasma frequency, scattering time), it is possible to determine some properties of this unusual system: the effective mass, the Fermi velocity, the Fermi energy, the room-temperature conductivity along the chains' directions and an estimate of the anisotropy in the conductivity of this compound.

CHAPTER II

STRUCTURE OF THE COMPOUND

The structure consists of a tetragonal lattice of AsF_6^- octahedra belonging to the space group $I4_1/amd$. This lattice contains linear, non-intersecting channels running along the a and b directions ($a = b \neq c$). The mercury atoms form chains within these channels. The Hg-Hg distance along these chains is incommensurate with the tetragonal lattice parameter a and is smaller than in elemental mercury. The position of the mercury atoms within a given chain is also disordered with respect to the position in adjacent chains. However, the chains still fulfill the crystal symmetry requirements if one considers them as rods of uniform density. An isometric view of the structure is shown in Fig. 1.

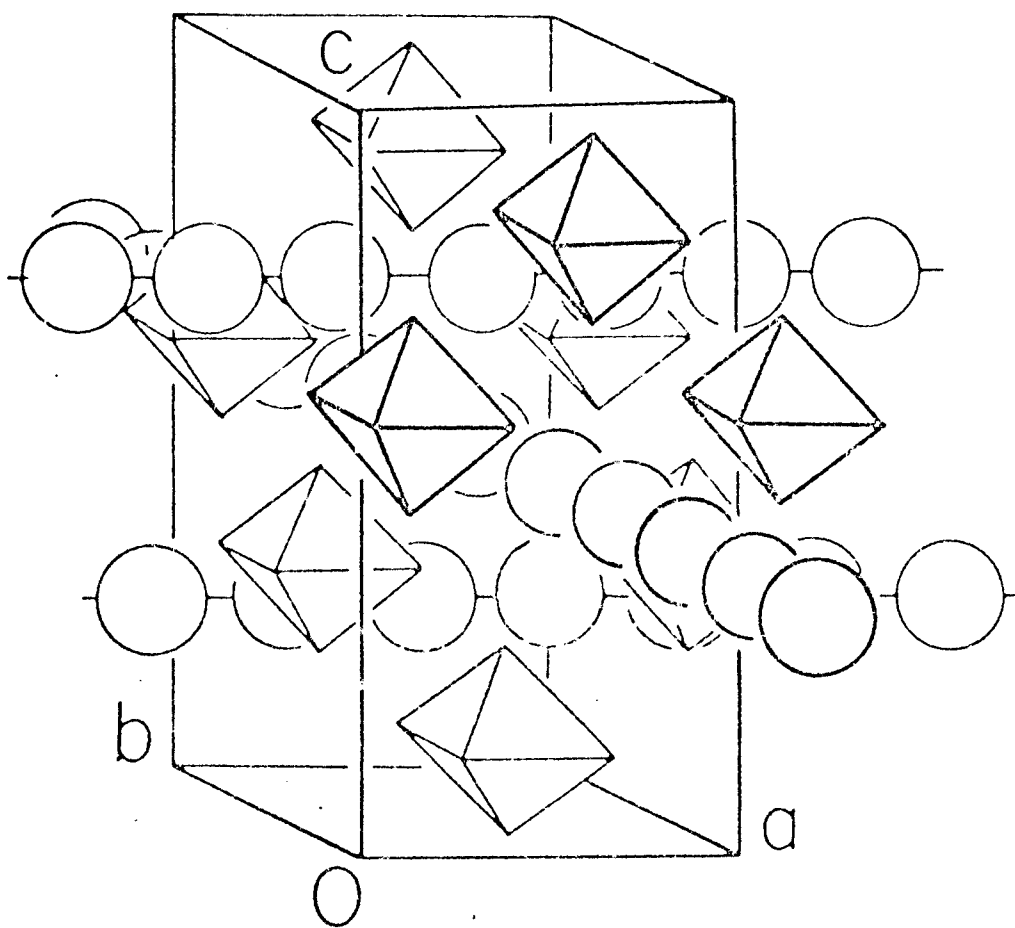
The values of the unit cell parameters were obtained from careful X-ray analysis (Brown *et al.*, 1974) using intensity measurement of the Bragg peaks on a syntex p1 four circle autodiffractometer. The Hg-Hg distance along the chains was determined from an analysis of sheets of diffuse intensity on precession photographs. The crystal data are summarized in Table 1.

TABLE 1

CRYSTAL DATA FOR $\text{Hg}_{2.86}\text{AsF}_6$

| System | Tetragonal |
|--|----------------------|
| Cell constants | |
| a | 7.538 Å |
| c | 12.339 Å |
| Number of formula units per unit cell | 4 |
| Cell volume | 701.1 Å ³ |
| Hg-Hg distance | 2.64 Å |
| Interchain separation | |
| along c | 3.085 Å |
| along a and b | 7.538 Å |

Figure 1: Isometric view of $\text{Hg}_{2.86}\text{AsF}_6$ showing the chains of mercury atoms (circles) running through the lattice composed of AsF_6^- ions (octahedra).



CHAPTER III

THEORY OF OPTICAL REFLECTION

Reflection occurs when light incident on a surface at a certain angle returns from this surface at the same angle with respect to the normal. Conditions of continuity at the surface separating the two media can provide the relations between the amplitude of the oscillating electric and magnetic field of the electromagnetic wave in the incident, reflected and transmitted wave. These boundary conditions give two sets of Fresnel equations depending on whether the electric field is polarized parallel or perpendicular to the plane of incidence (plane containing the incident and reflected beam). For non-magnetic materials, these equations are

$$(E_r/E_i)_\perp = \frac{n_1 \cos \theta_i - n_2 \cos \theta_t}{n_1 \cos \theta_i + n_2 \cos \theta_t} \quad (1)$$

$$(E_r/E_i)_\parallel = \frac{n_1 \cos \theta_t - n_2 \cos \theta_i}{n_1 \cos \theta_t + n_2 \cos \theta_i} \quad (2)$$

where r stands for reflected beam and i for incident beam; θ_i , θ_t are the angles of incidence and of refraction; n_1 , n_2 are the indices of refraction for the two media.

For reflection at the interface of air, n_1 is one, and for a metal, the wave is rapidly attenuated inside the metal (therefore, θ_t is approximately zero). This implies that the reflection coefficient is

given by

$$R_{\perp} = \left| \frac{\cos\theta_i - n}{\cos\theta_i + n} \right|^2 \quad (3)$$

$$R_{||} = \left| \frac{1 - n\cos\theta_i}{1 + n\cos\theta_i} \right|^2 \quad (4)$$

The index of refraction is related to the dielectric constant, ϵ

$$n^2 = \epsilon \quad (5)$$

The dielectric constant itself is related to the polarizability of the crystal, α

$$\epsilon = 1 + 4\pi N\alpha \quad (6)$$

The following theory has been described by F. WOOTEN in "Optical Properties of Solids" (1972).

The polarizability is a measure of how much the constituents of the crystal react to the varying electric field created by the incident light. There are two simple models that look at the way the electrons in the crystal behave in the presence of the varying field. The first one considers that the electrons are bound to the nucleus in much the same way as a small mass can be bound to a large mass by a spring. This is the Lorentz model. The second one considers that the electrons are completely free. It is the Drude model. They give the complex dielectric constants as functions of the frequency, ω . The Lorentz model gives

$$\hat{\epsilon} = 1 + \frac{4\pi e^2}{m} \sum_J \frac{N_J}{(\omega_J^2 - \omega^2) - i\Gamma_J\omega} \quad (7)$$

where N_J is the density of electrons bound with resonant frequency ω_J ;

Γ_J is a measure of the damping of the oscillation and e , m are respectively the charge and mass of the electron. For one resonant frequency, ω_0

$$\text{Re } \hat{\epsilon} = \epsilon_1^L = 1 + \frac{4\pi N e^2}{m} \frac{\omega_0^2 - \omega^2}{(\omega_0^2 - \omega^2)^2 + \Gamma^2 \omega^2} \quad (8)$$

$$\text{Im } \hat{\epsilon} = \epsilon_2^L = \frac{4\pi N e^2}{m} \frac{\Gamma \omega}{(\omega_0^2 - \omega^2)^2 + \Gamma^2 \omega^2} \quad (9)$$

The Drude model gives

$$\hat{\epsilon} = 1 - \frac{4\pi N e^2}{m(\omega^2 + i\omega/\tau)} \quad (10)$$

where τ is the mean time between collisions for the free electrons. It is the same scattering time used in the dc conductivity

$$\sigma_0 = \frac{N e^2 \tau}{m} \quad (11)$$

The plasma frequency is defined as the frequency of natural oscillation of the gas of electrons of the same density, N

$$\omega_p^2 = \frac{4\pi N e^2}{m} \quad (12)$$

The dielectric constant becomes

$$\epsilon_1^D = 1 - \frac{\omega_p^2 \tau^2}{(1 + \omega^2 \tau^2)} \quad (13)$$

$$\epsilon_2^D = \frac{\omega_p^2 \tau^2}{\omega(1 + \omega^2 \tau^2)} \quad (14)$$

From the real and imaginary part of the dielectric constant and

$$\hat{n} = n + ik \quad (15)$$

one obtains from Eq. 5

$$n = \left\{ \frac{1}{2} [(\epsilon_1^2 + \epsilon_2^2)^{\frac{1}{2}} + \epsilon_1] \right\}^{\frac{1}{2}} \quad (16)$$

$$k = \left\{ \frac{1}{2} [(\epsilon_1^2 + \epsilon_2^2)^{\frac{1}{2}} - \epsilon_1] \right\}^{\frac{1}{2}} \quad (17)$$

The reflectivity is then given by

$$R_{\perp} = \frac{(n - \cos\theta_i)^2 + k^2}{(n + \cos\theta_i)^2 + k^2} \quad (18)$$

$$R_{\parallel} = \frac{[n - (1/\cos\theta_i)]^2 + k^2}{[n + (1/\cos\theta_i)]^2 + k^2} \quad (19)$$

The characteristics of the reflection spectra for both models are the following. In the Drude model, the reflectivity is close to zero for frequencies higher than the plasma frequency. Then, at the plasma frequency, it rises to a high value over a frequency range inversely proportional to τ . It keeps increasing slowly toward one at low frequencies.

For the Lorentz oscillator model, the reflectivity is low at low frequency. It rises to a high value over a range of Γ_J around the resonant frequency ω_J . It then returns to a low value for frequencies higher than the plasma frequency

$$\omega_{pJ}^2 = \frac{4\pi N_J e^2}{m} \quad (20)$$

which is not the same as the free electron plasma frequency and does not

correspond to a natural excitation of the electrons.

Both the Drude and Lorentz models can be used in analysing the reflectivity of a metal since the free electrons in the metal will behave according to the Drude model replacing the free electron mass by the effective mass and transitions between the valence and the conduction bands will present the same form as Lorentz oscillators.

However, a model more appropriate to quasi-one-dimensional metal has been presented by Rice and Bernasconi (1972) to replace the Drude model. It is a phenomenological theory based on a model of linear metallic strands interrupted by insulating lattice defects. Two relaxation times, τ_o and τ_R , are used to derive an expression for the dielectric constant. τ_o denotes a relaxation time characteristic of the "intrinsic" conductivity of the defect free strands while τ_R specifies a mean time for the build-up of space charge polarization effects at a constricting defect. They then obtained, for the dielectric constant, the formula

$$\epsilon(\omega) = 1 + \frac{\lambda \omega_p^2 \tau_R^2}{(1 - i\omega\tau_R)^\lambda (1 - i\omega\tau_o)} \quad (21)$$

where

$$\lambda = \frac{\tau_o}{\tau_o + \tau_R} \quad (22)$$

and

$$\omega_p^2 = 4\pi n_a (v/a) e^2 / m^* \quad (23)$$

where n_a is the number of metallic strands per unit area perpendicular to the strand direction, v is the number of carriers per metal atoms,

a is the lattice spacing of the metallic strands, and m^* is the effective mass of the carriers.

The high-frequency dependence of the dielectric constant is similar to the Drude model. However, in the low frequency limit $\epsilon_2(\omega)$ diverges as ω^{-1} in the Drude model whereas in the present model $\epsilon_2(\omega)$ approaches zero as ω giving rise to a purely real static dielectric constant. Finally, the reflectivity does not approach unity in the low frequency limit and the absorption is proportional to ω^2 rather than $\omega^{\frac{1}{2}}$ as in the Drude model in the same limit.

In the limit $\tau_0 \gg \tau_R$ ($\lambda \rightarrow 1$) which is reasonable for our compound since the conductivity anisotropy is large, the dielectric constant becomes

$$\epsilon(\omega) = 1 + \frac{\omega_p^2 \tau_R^2}{(1 - i\omega\tau_R)^2} \quad (24)$$

In the range $\omega\tau_R \gg 1$, this model gives values close to the Drude model if one replaces τ by τ_R .

From the plasma frequency, ω_p , an estimate of the carrier effective mass can be made. Using the one dimensional Fermi wavevector

$$k_F = (v\pi/2a) \quad (25)$$

one can obtain the Fermi velocity

$$v_F = \hbar k_F / m^* \quad (26)$$

and the Fermi energy

$$\epsilon_F = \frac{1}{2} m^* v_F^2 \quad (27)$$

Since the scale of τ_R is fixed by the time taken for a carrier

to traverse the mean distance between defects, λ_0 ,

$$\tau_R \sim \frac{\lambda_0}{v_F} \quad (28)$$

This estimate of λ_0 gives an anisotropy of the conductivity of about $(\lambda_0/d)^2$ where d is the lateral separation of the strands.

This is valid for an isotropic crystal having metallic properties. Since this compound is strongly anisotropic with tetragonal symmetry, one must use a dielectric tensor of the form

$$\epsilon = \begin{vmatrix} \epsilon_{ab} & 0 & 0 \\ 0 & \epsilon_{ab} & 0 \\ 0 & 0 & \epsilon_c \end{vmatrix} \quad (29)$$

with respect to axis a , b and c , where a and b are the high conductivity directions, while c is the low conductivity direction.

If we look at reflection off the ab face, the crystal behaves like an isotropic sample with dielectric constant ϵ_{ab} .

However, the other plane accessible for a reflection experiment is the $1\bar{2}3$ plane, where $1\bar{2}3$ is a system of axis obtained from the axis abc by a rotation of 25° with respect to the a axis. The axis 1 coincides with the axis a .

The dielectric tensor with respect to this new set of axis becomes

$$\epsilon = \begin{vmatrix} \epsilon_{ab} & 0 & 0 \\ 0 & \epsilon_{ab} \cos^2 \phi + \epsilon_c \sin^2 \phi & \sin \phi \cos \phi (\epsilon_c - \epsilon_{ab}) \\ 0 & \sin \phi \cos \phi (\epsilon_c - \epsilon_{ab}) & \epsilon_{ab} \sin^2 \phi + \epsilon_c \cos^2 \phi \end{vmatrix} \quad (30)$$

where

$$\phi = 25^\circ$$

Using the continuity equations at the interface between the media and taking the 23 plane as the plane of incidence, we then get

$$(E_r/E_i)_\perp = - \frac{1 - \xi_{11} \cos \theta_i}{1 + \xi_{11} \cos \theta_i} \quad (31)$$

$$(E_r/E_i)_{||} = - \frac{\cos \theta_i - \xi_{22}}{\cos \theta_i + \xi_{22}} \quad (32)$$

where

$$\xi_{11}^2 = 1/\epsilon_{ab} \quad (33)$$

$$\xi_{22}^2 = \frac{\cos^2 \phi}{\epsilon_c} + \frac{\sin^2 \phi}{\epsilon_{ab}} \quad (34)$$

Therefore, reflection with the polarization perpendicular to the plane of incidence is the same for both faces, and reflection on the 13 plane with the electric field in the plane of incidence is a function of a combination of the dielectric constants for the high and low conductivity direction.

CHAPTER IV

EXPERIMENTAL METHOD

A. Sample Preparation

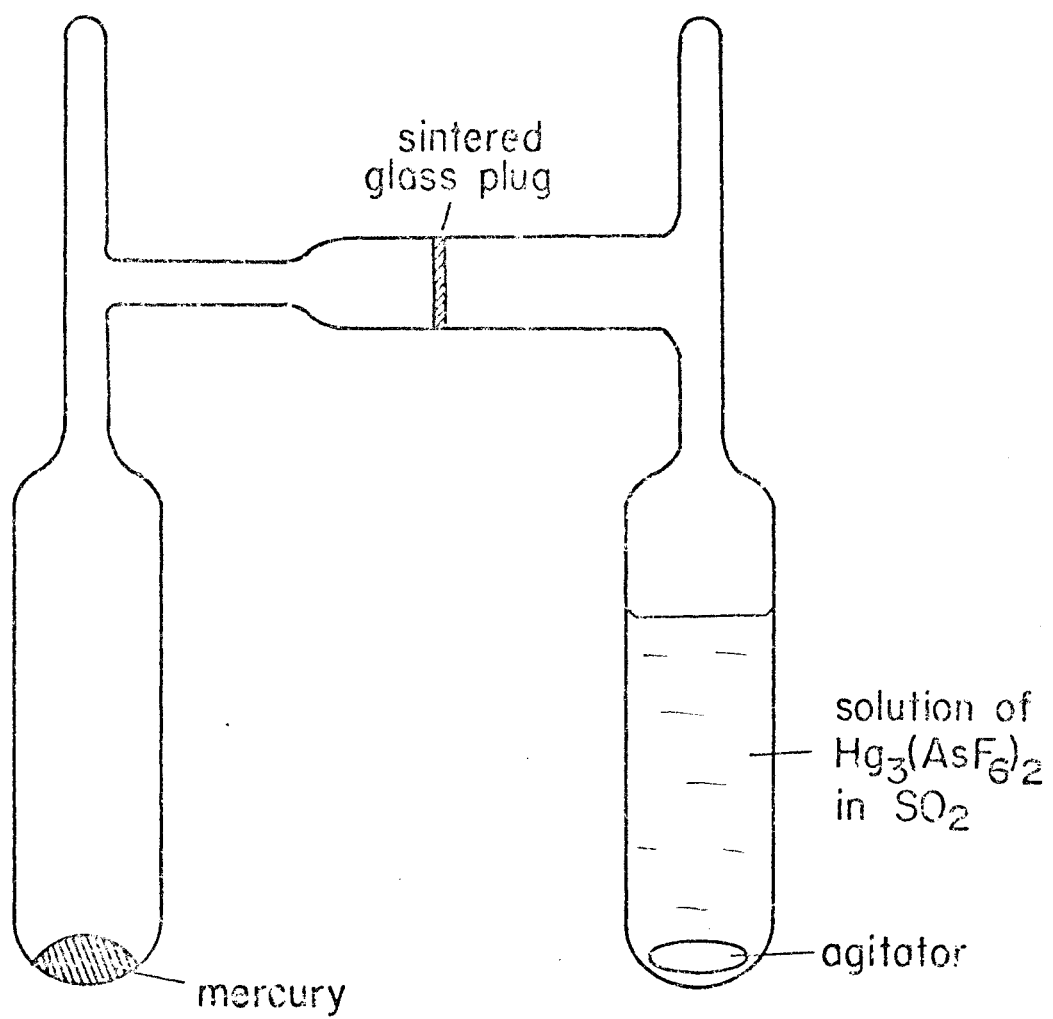
The sample was prepared using a technique developed by B. Cutforth (Cutforth et al, 1975). Crystals were grown in a special test tube illustrated in Fig. 2. A solution of $\text{Hg}_3(\text{AsF}_6)_2$ in liquid SO_2 was prepared on one side of the test tube while a small amount of elemental mercury was put on the other side. After cooling to -35°C , the solution was transferred onto the mercury. The crystals grew on the mercury surface while the temperature was maintained at -35°C until most of the mercury had gone into the reaction. The solution was then transferred back into the other side of the test tube. The compound was separated from the rest of the mercury and washed with condensed SO_2 . The largest crystals had surfaces of approximately 10 mm^2 .

B. Apparatus

These mercury compounds are highly hygroscopic, hence, they cannot be handled directly in the atmosphere. The crystals were mounted in quartz tubes inside a dry box with the desired face parallel to the tube walls. The samples were held in place by glasswool that had been thoroughly dried. The atmosphere inside the tube was high purity dry nitrogen at room pressure.

The quartz tube is fixed on a goniometer that permits one to turn

Figure 2: Test tube used for sample preparation.



the sample with respect to two axis. The light from a small source is focused on the sample at an angle of 22° . The reflected beam is focused on the entrance slit of a Czerny-Turner monochromator after passing through a polarizer and a filter. (Fig. 3)

The Czerny-Turner spectrometer is a grating-type monochromator. The incident light after passing through the slit is reflected by an aspherical mirror on the grating. The beam reflected from the grating at the angle corresponding to a particular wavelength is reflected onto a second aspherical mirror that focuses it onto the exit slit. The appropriate detector can be screwed on this slit. An opening on the top of the spectrometer and an easy lock-in mechanism made it possible to interchange gratings rapidly.

A chopper placed in front of the source was used to modulate the signal at a frequency of 20 Hz. The voltage from the detector was pre-amplified and fed into a phase sensitive detector where it was compared to the reference signal from a solar cell placed on the base of the first focusing lens.

To measure reflectivity over a wide range in wavelength, it was necessary to use filters to limit the reflection from the grating to the first order. We also used two sources, three types of polarizers, two gratings and two detectors. The different ranges and the corresponding combinations of source, polarizer, filter, grating and detector are given in Table 2.

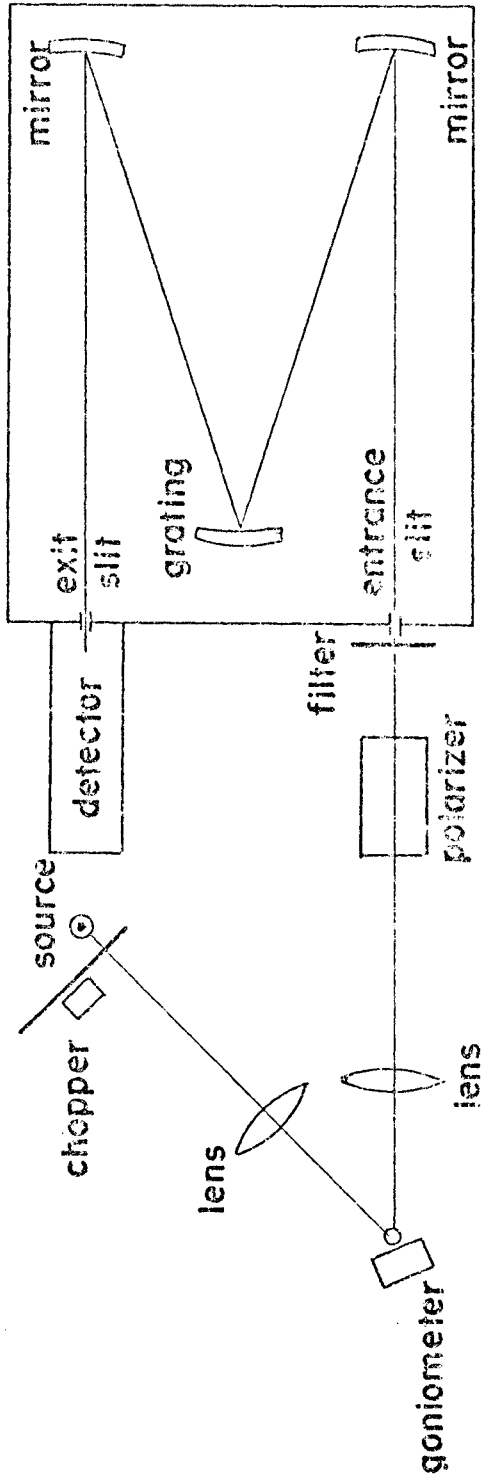
Absorption from the lenses, the quartz tube, the polarizer and the filter, and the response of the grating to different types of polarization (with respect to the grating rulings) make it impossible to

TABLE 2

EXPERIMENTAL COMPONENTS FOR ALL FREQUENCY RANGES

| Range (Microns) (eV) | Source | Polarizer | Filter | Grating | Detector |
|----------------------------|---------------|--|-----------|-----------|-------------------|
| 0.3 - 0.5 2.5 - 4.1 | Hydrogen lamp | Ultraviolet | Glass | 0.5 μ | Photomultiplier |
| 0.4 - 0.8 1.6 - 3.1 | Tungsten lamp | Visible | Yellow | 0.5 μ | Photomultiplier |
| 0.7 - 1.4 0.89 - 1.8 | Tungsten lamp | Infrared | - | 0.5 μ | Lead sulfide cell |
| 1 - 2 0.62 - 1.2 | Tungsten lamp | Infrared | - | 1.6 μ | Lead sulfide cell |
| 1.8 - 2.7 0.46 - 0.69 | Tungsten lamp | Infrared | Germanium | 1.6 μ | Lead sulfide cell |
| 1.8 - 3.6 0.34 - 0.69 | Tungsten lamp | - | Germanium | 1.6 μ | Lead sulfide cell |
| 2.4 - 3.6 0.34 - 0.52 | Tungsten lamp | Plate polarizer (group of dielectric plates stacked at a certain angle) | Germanium | 1.6 μ | Lead sulfide cell |

Figure 3: Top-view of the reflectivity apparatus.



measure directly the reflectivity. By replacing the sample by an aluminum mirror and looking at the reflection over the same ranges, it is possible using the ratio of the two signals to get a relative spectrum of the reflectivity.

A measurement of the absolute reflectivity at one wavelength is done inside a dry box. The beam produced by a He-Ne laser passes through a window of the dry box, is reflected by a mirror to fall on a lens that focuses it on the sample. The sample holder is fixed to a rotating rod that permits adjustment of the angle of reflection so that the reflected beam falls on a silicone solar cell situated between the lens and the sample. A measurement of the intensity of the direct laser beam completes this measurement of the absolute reflectivity at 6328 Å.

CHAPTER V

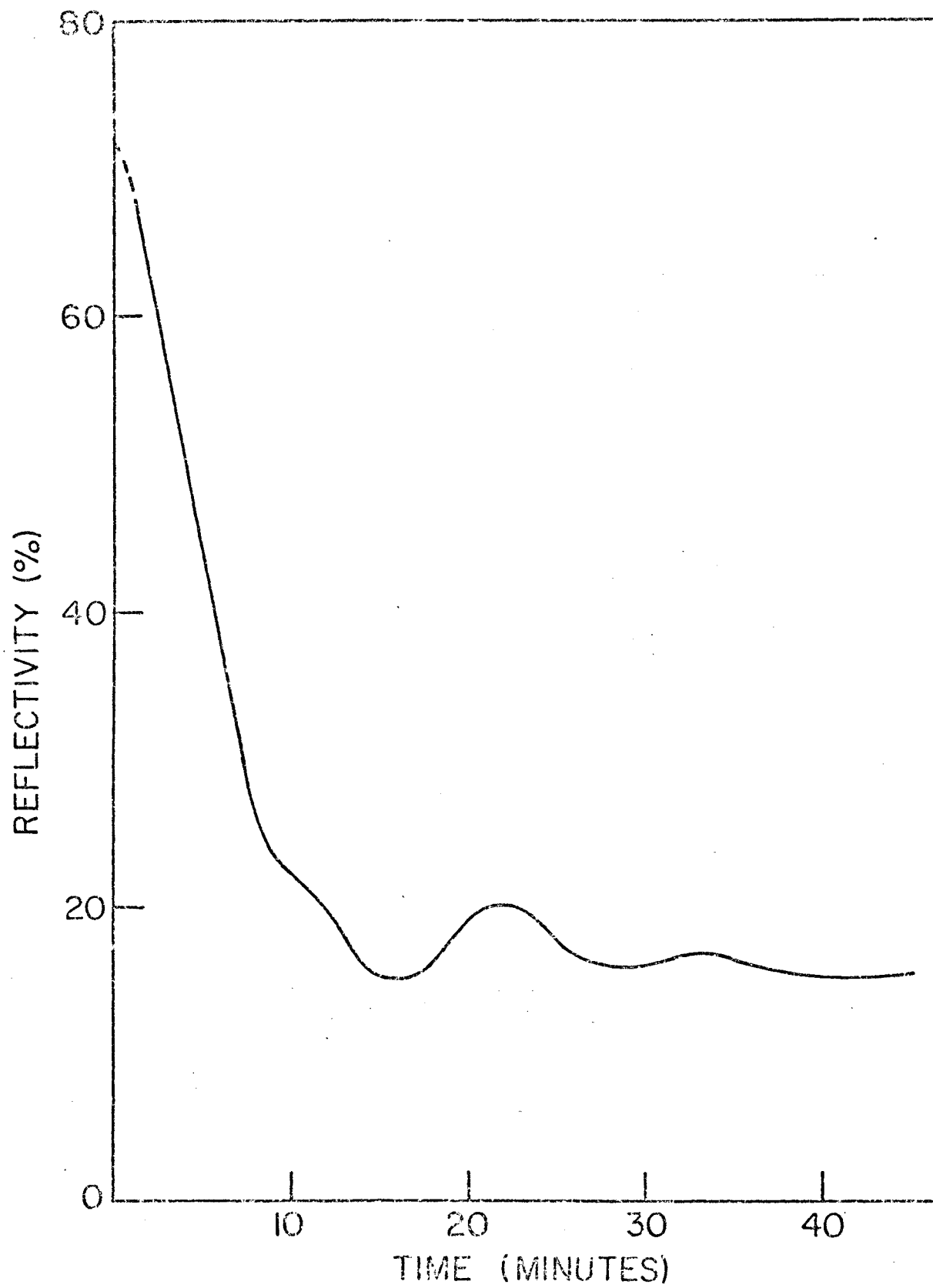
RESULTS

A. Experimental

The measurement of the absolute reflectivity was done inside the dry box using a disc plate of the sample having a diameter of 15 mm and a thickness of 1 mm grown from a slight variation of the method described before (the mercury was in contact with the SO_2 solution through a capillary). A value of $71 \pm 4\%$ was obtained for the reflectivity. It was possible to monitor the decomposition of the sample inside the dry box by measuring the time dependence of the reflectivity for about one hour (Fig. 5). The reflectivity decreases by a factor of five in 15 minutes. It also shows a maximum after 20 minutes which is tentatively attributed to the formation of a uniform coating of mercury on the surface of the crystal.

This emphasizes the necessity of measuring the reflectivity spectra of the crystals as soon as they are mounted and as fast as possible. Measurement of the whole spectrum usually took about five hours. However, the decomposition inside the quartz tubes is believed to be much slower than in the dry box since the total amount of water vapor, that contributes to the decomposition process, in the tube's atmosphere is much smaller than that in the dry box and once this limited amount of water vapor has reacted with the compound only the nitrogen is left, and the decomposition process is stopped. At the end of each experiment, the crystals still had lustrous

Figure 4: Reflectivity as a function of time in
the dry box.



faces.

Depending on the time spent mounting the crystal in the dry box, the quality of the results is expected to vary considerably. The reflectivity of eight different crystals was studied. Five of the samples were isotropic ab faces (AS1, AS2, AS3, AS4, AS5) and the other three were anisotropic faces (AS6, AS7, AS8). The anisotropic face is the 13 plane where the axis 1 is identical to a and 3 is the c axis rotated by 25° with respect to a. For the first four, the reflectivity along the chain axis was measured with the electric field vector in the plane of incidence. The last three were studied with the electric field perpendicular to the plane of incidence. Spectra of the sample AS5 were taken with both directions of polarization. Finally, measurement of the reflectivity in the direction of axis 3, was done with the electric field in the plane of incidence for samples AS6, AS7 and AS8.

Since the total spectrum is composed of six different ranges, the reflectivity at the end of one range must be matched to the beginning of the next range. This is done by taking an average of the ratio of both ranges for all the overlapping frequencies. This gives the possibility of a systematic error if one of the matching ratios is not exact. Finally, the relative spectrum obtained in this way is scaled so that the reflectivity at 0.63μ is the one given by the absolute reflectivity measurement.

Among the eight samples studied, five (AS2, AS4, AS5, AS6, AS8) gave spectra with the same general features for the reflection along the mercury chains. The reflectivity is approximately constant at 70% for frequencies between 0.5 and 2.5 eV. Then, it decreases sharply and shows

a minimum at 3.5 eV. It rises slowly up to the end of the experimental range (about 4 eV) (Fig. 5). For the sample AS5, reflection spectra with both directions of polarization with respect to the plane of incidence show the same characteristics.

The reflectivity for light polarized along axis 3 was correctly measured for only one sample (AS6). It shows a peak at about 2.5 eV (the frequency at which the plasma edge occurs for the high conductivity direction) and is low for all other frequencies (Fig. 6).

B. Analysis

Since the data on reflectivity in the high conductivity direction for frequencies lower than the plasma edge presented some scattering (increasing for some crystals and decreasing for others), an average of the reflectivity at each frequency for all samples with the same polarization of the light was taken for frequencies lower than 2 eV. This average was then used for the range less than 2 eV in analyzing the spectrum of an individual sample.

The spectra were fitted using a Drude model and two Lorentz oscillators: one with a frequency lower than the plasma edge and one with a higher frequency. A computer programme was used to adjust the eight parameters involved in this model to the observed spectra using a least-squares procedure. The average of these eight parameters for the six spectra analyzed are the following:

$$\begin{aligned}\hbar\omega_p &= 5.80 \pm .34 \text{ eV} \\ \tau/\hbar &= 2.19 \pm .62 \text{ eV}^{-1} \\ \hbar\omega_{p1} &= 7.03 \pm .93 \text{ eV}\end{aligned}$$

Figure 5: Reflectivity spectrum for the light polarized along the high conducting direction. The open circles represent the experimental data. The continuous line is a Drude-Lorentz fit with the following parameters:

$$\hbar\omega_p = 5.26 \text{ eV}$$

$$\tau/\hbar = 2.75 \text{ eV}^{-1}$$

$$\hbar\omega_{p1} = 6.32 \text{ eV}$$

$$\tau_1/\hbar = 1.52 \text{ eV}^{-1}$$

$$\hbar\omega_{o1} = 5.15 \text{ eV}$$

$$\hbar\omega_{p2} = 2.08 \text{ eV}$$

$$\tau_2/\hbar = 1.77 \text{ eV}^{-1}$$

$$\hbar\omega_{o2} = 1.51 \text{ eV}$$

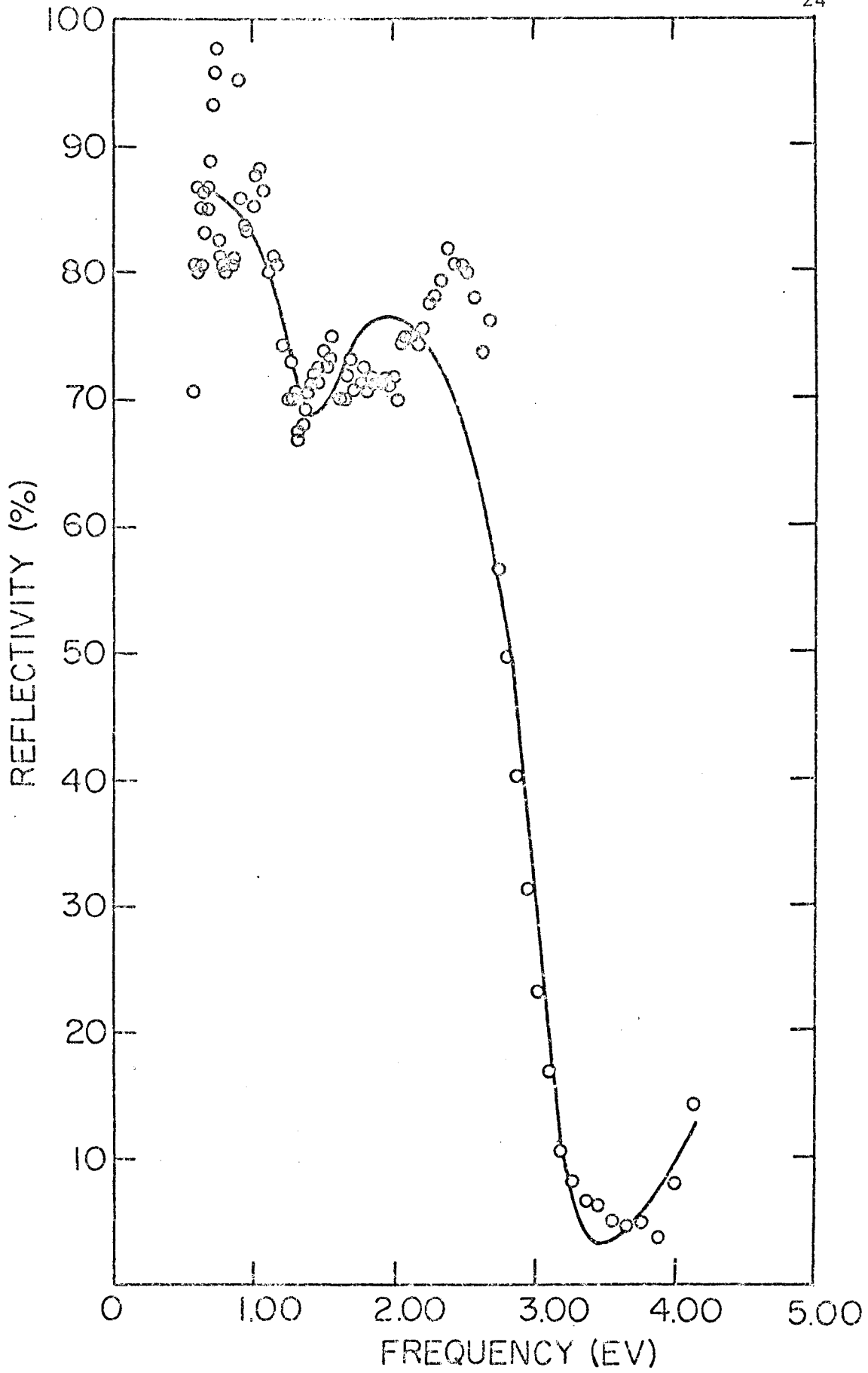
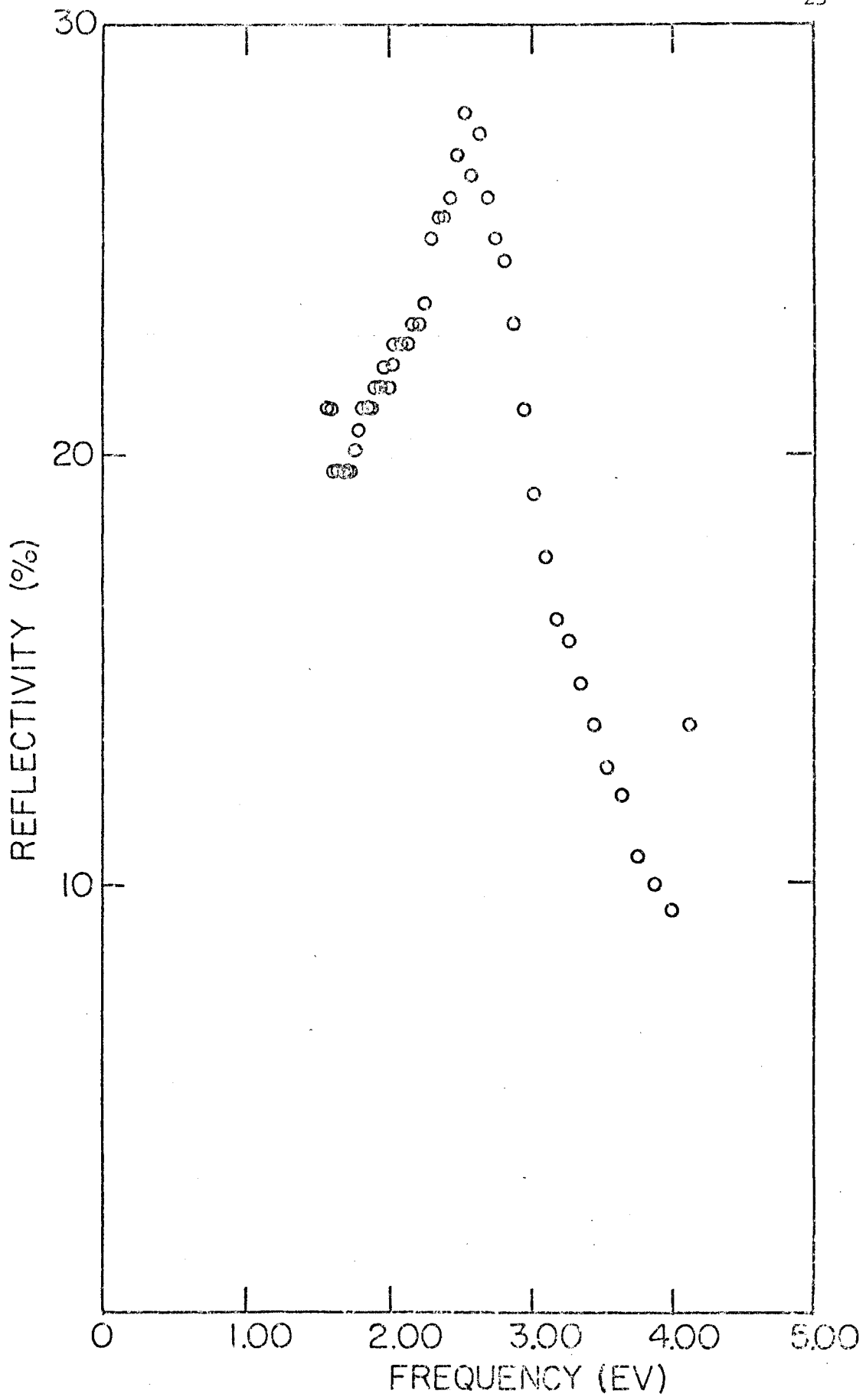


Figure 6: Reflectivity spectrum for light polarized
along axis 3.



$$\tau_1/\hbar = 5.73 \pm 3.91 \text{ eV}^{-1}$$

$$\hbar\omega_{o_2} = 4.64 \pm .24 \text{ eV}$$

$$\hbar\omega_{p_2} = 5.99 \pm 1.11 \text{ eV}$$

$$\tau_2/\hbar = 1.13 \pm .20 \text{ eV}^{-1}$$

$$\hbar\omega_{o_2} = 1.32 \pm .12 \text{ eV}$$

giving a dc conductivity of $9.89 \times 10^3 (\Omega \times \text{cm})^{-1}$. The average of $\sqrt{\chi^2}$ for these fits is 0.52. This corresponds to an average deviation of 5% between the theoretical and experimental curves.

CHAPTER VI

DISCUSSION

The value of the plasma frequency obtained from the fit does not correspond to the frequency of the plasma edge in the actual spectra. This is because the plasma edge occurs when the real part of the dielectric constant goes through zero. In the Drude model, this happens at the plasma frequency if $\omega_P \tau \gg 1$. However, the Lorentz oscillator at a frequency close to the plasma frequency (4.64 eV) shifts the position where $\epsilon = 0$ to a lower frequency.

The peak at the frequency of the plasma edge in the spectrum for light polarized along axis 3 appears because this axis is 25° from the c axis and the reflection is not strictly specular (angle of incidence $\neq 0$). This is predicted by Bulaevski and Kukharensko (1973) for quasi two dimensional crystals.

No physical significance is attached to either Lorentz oscillator since a band structure calculation has not been done. Therefore, these Lorentz oscillators cannot be assigned to any particular transitions.

The value obtained for the dc conductivity from the plasma frequency and the scattering time is in good agreement with the value obtained from electrical measurements (about $10^4 (\Omega \times \text{cm})^{-1}$).

Furthermore, from the plasma frequency, it is possible to get v/m^* since all the other parameters in the definition of the plasma frequency (Eq. 23) are known from the X-ray analysis.

The intermercury distance along the chains being much smaller than in the metal, one expects considerable overlap of the atomic orbitals. The 5d orbitals are split by the crystal field of the AsF_6^- anions. This splitting may cause an overlap between the highest crystal-split d-orbital and the $6s^2$ and 6p orbitals forming a conduction band. However, it should be stressed that energy band calculations are needed to confirm this overlap model.

According to this model, the number of free carrier per mercury atoms would be 3.65 electrons since 0.35 electrons are given to the AsF_6^- group by each mercury atom. From this the following quantities are determined.

$$\begin{aligned} m^* &= 0.84 \pm .11 m_e \\ k_F &= 2.17 \pm .02 \times 10^8 \text{ cm}^{-1} \\ v_F &= 2.98 \pm .42 \times 10^8 \text{ cm/sec} \\ \epsilon_F &= 21.2 \pm 3.2 \text{ eV} \end{aligned}$$

v_F is the only property that does not depend on the value of the number of free carriers per atom. The value for the effective mass is rather close to that of the free electron mass. As Brüesch (1975) has pointed out, the free electron mass should be a characteristic value for charge carriers in one-dimensional systems.

Finally, from the model of Rice and Bernasconi of metallic strands interrupted by insulating lattice defects, the parameter τ in the Drude model is really τ_R . This provides an estimate of the average distance between defects, $\ell_o = v_F \tau_R = 43 \text{ \AA}$. And since $b = 3.085 \text{ \AA}$, the anisotropy, $(\ell_o/d)^2$, is estimated to be about 190. This is of the same order of magnitude as the anisotropy observed in the electrical measurements.

Since the compounds $\text{Hg}_{2.86}\text{AsF}_6$ and $\text{Hg}_{2.91}\text{SbF}_6$ are isostructural, it is expected that their physical properties should be similar. However, comparison of the reflectivity spectrum for the arsenic compound to the data obtained by Koteles et al (1976) for the antimony compound shows substantial differences. The fitted plasma frequency for the antimony compound is smaller by a factor of about two and the frequency of the two Lorentz oscillators differ markedly from the ones for the present set of results. It is believed that this is due to an underestimate of the reflectivity of $\text{Hg}_{2.91}\text{SbF}_6$ at $0.63\ \mu$. The value of 35% obtained for this compound is much lower than the reflectivity of 71% of $\text{Hg}_{2.86}\text{AsF}_6$ for the same wavelength. In addition, the increase of the reflectivity in the infrared may be attributed to a possible error in the matching ratios between frequency ranges. If these two errors are corrected, both spectra become very similar as expected.

CHAPTER VII

CONCLUSION

The reflection from $\text{Hg}_{2.86}\text{AsF}_6$ has been found to be highly anisotropic showing a plasma edge in the high-conductivity direction but being constant at a low value in the direction of axis 3. The value of the dc conductivity in the direction of axis a and b has been confirmed by the parameters in the Drude model fitted to the spectra together with two Lorentz oscillators. Also, the theory of Rice and Bernasconi has been shown to give a value for the conductivity anisotropy in the same order of magnitude as the one observed. However, measurement of the reflectivity in the far infrared would be a better test for this theory. Two interesting conclusions from this theory should be pointed out. First, by reducing the number of lattice defects in the crystal, the conductivity anisotropy could be increased to a value such that the compound would become a true one-dimensional conductor. Secondly, by controlling the concentration of defects in the crystal, a wide range of values for the static dielectric constant could be obtained.

BIBLIOGRAPHY

- Brown, I. D., B. D. Cutforth, C. G. Davies, R. J. Gillespie, P. R. Ireland and J. E. Vekris, *Can J. Chem.* 52, 791, 1974.
- Brüesch, P., One-dimensional conductors, Lecture notes in physics 34, ed. by H. G. Schuster. New York: Springer-Verlag, 1975, p. 194.
- Bulaevski, L. N. and Y. A. Kukhareno, *Soviet Physics Solid State* 14, 2076, 1973.
- Cutforth, B. D., W. R. Datars, R. J. Gillespie and A. van Schyndel, Inorganic compounds with unusual properties, Advances in Chemistry series 150, ed. by R. B. King. Washington: American Chemical Society, 1975, p. 56.
- Cutforth, B. D., W. R. Datars, A. van Schyndel and R. J. Gillespie, *Solid State Commun.*, (to be published), 1976.
- Koteles, E. S., W. R. Datars, B. D. Cutforth and R. J. Gillespie, International conference on semi-conductors (Rome), 1976.
- Little, W. A., *Phys. Rev.* 134, A1416, 1964.
- Rice, M. J. and J. Bernasconi, *J. Phys. F. Metal Phys.* 2, 905, 1972.
- Schuster, H. G. editor, One-dimensional conductors, Lecture notes in physics 34. New York: Springer-Verlag, 1975.
- van Schyndel, A., W. R. Datars, B. D. Cutforth and R. J. Gillespie, (to be published) 1976.
- Wooten, F., Optical Properties of Solids. New York: Academic Press, 1972.